


# Effective parameters of a metamaterial composed of dielectric coated conducting cylindrical rods

Z. A. Awan , Hassan Ullah, Ahsan Ullah and Afshan Ashraf

Department of Electronics, Quaid-i-Azam University, Islamabad, Pakistan

## Research Paper

**Cite this article:** Awan ZA, Ullah H, Ullah A, Ashraf A (2020). Effective parameters of a metamaterial composed of dielectric coated conducting cylindrical rods. *International Journal of Microwave and Wireless Technologies* **12**, 797–808. <https://doi.org/10.1017/S1759078720000094>

Received: 9 October 2019

Revised: 21 January 2020

Accepted: 21 January 2020

First published online: 19 February 2020

### Key words:

Scattering; metamaterial; cylindrical rod; effective permittivity; effective permeability

### Author for correspondence:

Z. A. Awan [zeeshan@qau.edu.pk](mailto:zeeshan@qau.edu.pk)

## Abstract

In the first part, the scattering characteristics of an isolated dielectric coated conducting rod have been investigated. The types of considered coatings for the scattering analysis are realistic materials including barium strontium titanate, magnetodielectric, gallium arsenide, and silicon carbide. It is found that the gallium arsenide coating can be used to significantly reduce the scattering from a thin perfectly electric conducting cylindrical rod at specific observation angles. In the second part, the effective permittivity and permeability of metamaterials composed of two dimensional periodic arrangements of these dielectric coated conducting cylindrical rods have been studied. An increase in the double negative (DNG) bandwidth of a metamaterial composed of barium strontium titanate coated conducting rods has been observed in contrast to the corresponding bandwidth of a metamaterial composed of only barium strontium titanate material rods. Also an additional plasmonic epsilon negative (ENG) bandwidth has been found in case of a metamaterial composed of barium strontium titanate coated conducting rods. It is further studied that the widest ENG, mu negative, and DNG bandwidths exist for a metamaterial composed of gallium arsenide rods.

## Introduction

Recently, there has been a great deal of interest in the physics and engineering of metamaterials due to their important technical applications, see for example [1–23]. The concept of a metamaterial has been introduced by Veselago in 1967 [1]. He suggested a new type of material which has simultaneously negative permittivity and permeability. He also presented general properties of electromagnetic wave propagation in such a material. He theoretically created a lossless metamaterial and showed the extraordinary properties of this material which is not found in nature. Following the work of Veselago *et al.* theoretically studied the negative permittivity [2] material. They studied that an array of metallic wires with suitably chosen spacing and radius can be constructed to form a negative permittivity material. Pendry and his co-workers also proposed a negative permeability material based on the metallic split ring resonators [3]. Later on, Smith *et al.* proposed a metamaterial which shows simultaneously negative permittivity and permeability. They also carried out microwave experiments to test unusual properties of the metamaterial [4]. Shelby *et al.* performed first experiment to show negative refraction of the metamaterial which consists of two-dimensional array of repeated unit cells of copper strips and split ring resonators [5]. The word metamaterial shows that these materials do not exist in nature but they can be made artificially. These metamaterials can be classified as a single negative (SNG) and double negative (DNG) metamaterials [6]. The SNG metamaterial can be an epsilon negative (ENG) metamaterial or mu negative (MNG) metamaterial. The ENG metamaterial has real part of its effective permittivity as negative whereas the MNG metamaterial has real part of its effective permeability as negative. Likewise, the DNG metamaterial has real parts of its effective permittivity and effective permeability as negative simultaneously. The range of frequencies where the real part of the effective permittivity is negative can be defined as an ENG bandwidth. Similarly, the range of frequencies where the real part of the effective permeability is negative defines a MNG bandwidth. The range of frequencies for which ENG and MNG bandwidths overlap gives rise to a DNG bandwidth.

Alu *et al.* [7] have studied that pairing of ENG and MNG slabs under certain conditions give some interesting features like resonance, tunneling, zero reflection, and transparency. Some other interesting potential applications of SNG and DNG metamaterials have been studied and discussed by Alu and Engheta [8], Engheta *et al.* [9], and Kshetrimayum [10]. Recently, Awan has studied the effects of ENG or MNG background metamaterials upon the reflection and transmission characteristics of a lossy wire grid [11] and the realization of a DNG metamaterial based upon the realistic material coated spherical particles [12]. It is known that a wire medium or metamaterial has spectrum of its effective permittivity as

plasmonic [13,14], i.e. it has negative permittivity from zero frequency to the plasma cutoff frequency. Based upon this, we have defined a plasmonic ENG negative bandwidth as the range of frequencies from zero to the plasma frequency. Contrary to this, there also exists another type of ENG metamaterial whose effective permittivity spectrum is resonant, see for example, [15–17]. This is because of the finite size of the inclusions forming an ENG metamaterial. In this case, it is found that the effective permittivity of such metamaterial is negative from resonance frequency to plasma frequency. We take this range of frequencies as a resonant ENG bandwidth. The disadvantage of the resonant ENG metamaterials is that they have narrow ENG bandwidth.

A metamaterial composed of dielectric rods has been studied by many authors [18–23]. Silveirinha has proposed the nonlocal homogenization theory for a periodic lattice composed of long thin  $\epsilon$ -negative rods [18]. He argued that spatial dispersion effects cannot be ignored in case of an electromagnetic crystal. Peng and co-workers [19] have analyzed the left-handed properties of a metamaterial composed of BST dielectric rods theoretically and experimentally. Later on, the effective permittivity and permeability of a metamaterial composed of BST rods have been studied theoretically by Vynck *et al.* [20]. They also derived mathematical expressions for the electric and magnetic dipole moments of a cylindrical rod based on Mie scattering coefficients. Anisotropic effects in a metamaterial composed of dielectric cylindrical rods have been investigated by Peng and co-workers [21] theoretically and they also verified their results numerically. According to them, anisotropic effects are introduced by turning the square lattice symmetry to the rectangular lattice. Li and Ling [22] have derived the expressions for effective permittivity and permeability of a rod array composed of water filled cylindrical rods. They also studied the transmission loss incurred by random heights and random positioning of rods forming a rod array. According to them, the randomizations have little effects on the behavior of a rod array at low frequencies. Valero and Vesperinas [23] have investigated the behavior of a metamaterial composed of ordered and disordered dielectric rods. They concluded that strong scattering by disordered rods extinguishes most of the incident energy and hence no negatively refracted forward beam is observed. Some of the authors have studied the electromagnetic characteristics of a metamaterial composed of dielectric coated conducting rods, e.g. [24,25]. Valagiannopoulos and Tretyakov have proposed a symmetric absorbers based upon a single infinite grating of perfectly conducting rods covered by ordinary dielectrics [24]. They also provided a realistic absorber design which have an absorption of 97%. A concept of digital metamaterial has been introduced by Giovampaola and Engheta based upon analytical and numerical study [25]. They have used cylindrical or spherical core-shell inclusions for their design. They also applied their proposed methodology to the design of various digital lenses. From all the references cited above, no one has studied the scattering characteristics along with the effective parameters of a metamaterial composed of dielectric coated conducting rods with realistic dielectric materials such as  $\text{Ba}_{0.5}\text{Sr}_{0.5}\text{TiO}_3$  (BST) dielectric, magnetodielectric, low loss gallium arsenide (GaAs), and silicon carbide (SiC). Likewise, comparative analysis of scattering characteristics and effective parameters of metamaterials composed of perfectly electric conducting (PEC), dielectric, and dielectric coated PEC rods based upon these realistic materials have not been reported previously. They are studied in the current paper.

In first section of the paper, we have analytically developed and studied the scattering characteristics of an isolated dielectric

coated conducting rod. The various types of realistic dielectric materials as mentioned above have been considered as coating materials for a dielectric coated PEC rod and rod materials for an uncoated rod. The scattering characteristics of a dielectric coated PEC rod is also compared with the PEC and realistic material rods having the same radii. During the study, it is found that the GaAs coating can be used to significantly reduce the scattering width of a small radius PEC cylindrical rod at specific observation angles. In this way, we can hide a thin cylindrical PEC rod from the incoming wave at these specific observation angles which find applications in the stealth technology. It is also studied that by increasing the inner core radius of PEC rod inside the magnetodielectric coated conducting rod, the forward scattering width can be reduced whereas its backward scattering width can be enhanced. Such a type of enhanced backscattering is of an interest for radar engineering problems. In the second part of the paper, effective parameters of a metamaterial composed of dielectric coated conducting rods have been studied. It is found that the widest plasmonic ENG bandwidth is observed for a metamaterial composed of PEC rods and the narrowest plasmonic ENG bandwidth exists for a metamaterial composed of magnetodielectric coated conducting rods. A % increase of 0.6135% in a DNG bandwidth for a metamaterial composed of BST coated conducting rods has been observed as compared to a metamaterial composed of only BST rods which were reported by Vynck *et al.* [20]. There also exists an additional plasmonic ENG bandwidth for a metamaterial composed of BST coated conducting rods. For a metamaterial composed of magnetodielectric rods there exists non-overlapping ENG and MNG bandwidths which implies that there is no DNG bandwidth. Contrary to this, it is analyzed that a metamaterial composed of magnetodielectric coated conducting rods has overlapping ENG and MNG bandwidths which gives rise to a relatively wider DNG bandwidth as compared to a DNG bandwidth of a metamaterial composed of BST coated PEC rods. Likewise, it is studied that the widest ENG, MNG, and DNG bandwidths are observed in case of a metamaterial composed of GaAs rods whereas there exists no DNG bandwidth for a metamaterial composed of GaAs coated conducting rods. In case of a metamaterial composed of SiC rods, we have only resonant ENG bandwidth whereas for a metamaterial composed of SiC coated conducting rods, we have resonant as well as plasmonic ENG bandwidths. For both of these metamaterials, there exists no MNG and DNG bandwidths. These above mentioned findings based upon the proposed theory signify the novelty of the current work and have not been studied previously. This proposed theoretical study is also helpful in designing of ENG, MNG, and DNG metamaterials based on coated or uncoated cylindrical rods.

### Scattering characteristics of an isolated dielectric coated conducting rod

An infinite length circular cylindrical rod made of a PEC material having radius  $a$  is considered. This cylindrical rod is coated with a dielectric or magneto-dielectric material. The electromagnetic parameters of the coating are  $\epsilon_c = \epsilon_o \epsilon_{rc}$  and  $\mu_c = \mu_o \mu_{rc}$  where  $\epsilon_o$  and  $\mu_o$  are the permittivity and permeability of the free space respectively. Likewise, the parameters  $\epsilon_{rc}$  and  $\mu_{rc}$  represent the relative permittivity and relative permeability of the coating material respectively. A word magneto-dielectric is used for those materials whose relative permeability is different from unity. An outer radius of the coating is taken to be  $b$  with coating

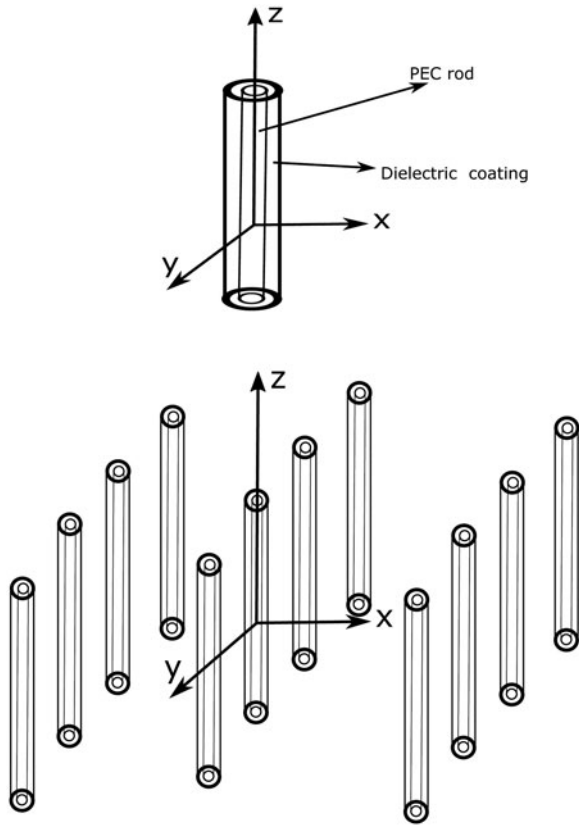


**Fig. 1.** The upper panel of the figure shows an isolated dielectric coated conducting cylindrical rod whereas the lower panel shows a medium composed of dielectric coated conducting rods.

thickness of  $\delta = b - a$ . The coating region has a propagation constant of  $k_c = k_o(\epsilon_{rc}\mu_{rc})^{1/2}$  and an intrinsic impedance of  $\eta_c = \eta_o(\mu_{rc}/\epsilon_{rc})^{1/2}$ . The factors  $k_o$  and  $\eta_o$  represent the free space propagation constant and the free space intrinsic impedance respectively. This dielectric coated cylindrical rod is placed in a certain background medium whose propagation constant is  $k_1 = k_o(\epsilon_{r1}\mu_{r1})^{1/2}$  and its intrinsic impedance is  $\eta_1 = \eta_o(\mu_{r1}/\epsilon_{r1})^{1/2}$ . It should be noted that a time convention of  $e^{j\omega t}$  has been assumed for the current study and suppressed throughout. The geometrical configuration of an isolated dielectric coated conducting rod has been given in the upper panel of Fig. 1.

This dielectric coated cylindrical rod is illuminated by a normal incident plane wave which travels in the direction that makes an angle  $\phi_o$  with the +x-axis. The incident wave polarization is taken to be transverse magnetic (TM) type whereas one can also extend this formulation for the transverse electric (TE) case. For the incident TM polarization, the z-component of the incident electric field  $E_z^i$  can be expressed as a sum of infinite cylindrical waves as follows [26,27],

$$E_z^i = E_o e^{-jk_o \rho \cos(\phi - \phi_o)} = E_o \sum_{n=-\infty}^{n=+\infty} j^{-n} J_n(k_o \rho) e^{jn(\phi - \phi_o)} \quad (1)$$

where  $E_o$  is a constant magnitude of the electric field. The function  $J_n(\cdot)$  represents an  $n$ th order Bessel function of first kind. The z-component of the scattered electric field  $E_z^s$  in the region

defined by  $0 \leq \phi \leq 2\pi$  and  $\rho > b$  can be written as,

$$E_z^s = E_o \sum_{n=-\infty}^{n=+\infty} j^{-n} C_n^{TM} H_n^{(2)}(k_o \rho) e^{jn(\phi - \phi_o)} \quad (2)$$

Likewise, the z-component of the electric field  $E_z^c$  inside the coating region which occupies the space defined by  $0 \leq \phi \leq 2\pi$  and  $a < \rho < b$  can be written as,

$$E_z^c = E_o \sum_{n=-\infty}^{n=+\infty} j^{-n} [A_n^{TM} J_n(k_c \rho) + B_n^{TM} Y_n(k_c \rho)] e^{jn(\phi - \phi_o)} \quad (3)$$

The factors  $A_n^{TM}$ ,  $B_n^{TM}$ , and  $C_n^{TM}$  are the unknown expansion coefficients and needed to be determined. Here  $Y_n(\cdot)$  is the  $n$ th order Bessel function of second kind and  $H_n^{(2)}(\cdot)$  is the  $n$ th order Hankel function of second kind which represents an outward traveling cylindrical wave. The  $\phi$ -components of the incident magnetic, scattered magnetic, and magnetic field inside the coating can be found from the Maxwell's equations. The unknown coefficients  $A_n^{TM}$ ,  $B_n^{TM}$ , and  $C_n^{TM}$  can be found by applying the tangential boundary conditions at interfaces  $\rho = a$  and  $\rho = b$  and solving the resulting system of linear equations. Once these unknowns become known then the z-components of the electric field in each region can be found from equations (1)–(3). The unknown coefficient  $C_n^{TM}$  which is of an interest for the scattered electric field can be found as below,

$$C_n^{TM} = - \frac{(1/\eta_c)J_n(k_1 b)P_n + (1/\eta_1)J'_n(k_1 b)Q_n}{(1/\eta_c)H_n^{(2)}(k_1 b)P_n + (1/\eta_1)H_n^{(2)'}(k_1 b)Q_n} \quad (4)$$

$$P_n = J'_n(k_c b)Y_n(k_c a) - J_n(k_c a)Y'_n(k_c b) \quad (5)$$

$$Q_n = J_n(k_c a)Y_n(k_c b) - J_n(k_c b)Y_n(k_c a) \quad (6)$$

where the prime ' shows the derivative with respect to the argument. If there exists no inner core of the perfectly conducting material then the scattering coefficient  $C_n^{TM}$  for a dielectric cylindrical rod of radius  $b$  using the above procedure can be written as,

$$C_n^{TM} = - \frac{(1/\eta_c)J_n(k_1 b)J'_n(k_c b) - (1/\eta_1)J_n(k_c b)J'_n(k_1 b)}{(1/\eta_c)J'_n(k_c b)H_n^{(2)}(k_1 b) - (1/\eta_1)J_n(k_c b)H_n^{(2)'}(k_1 b)} \quad (7)$$

In case if the cylindrical rod is made of a perfectly conducting material having radius  $b$  and placed in the free space background, i.e.  $k_1 = k_o$  then the scattering coefficient  $C_n^{TM}$  can be written as follows,

$$C_n^{TM} = - \frac{J_n(k_o b)}{H_n^{(2)}(k_o b)} \quad (8)$$

In this case, it is assumed that the cylindrical rod have finite conductivity  $\sigma_c$  which shows that the permittivity  $\epsilon_c$  is a complex quantity with an imaginary part of  $\sigma_c/j\omega$ . Now by taking  $\sigma_c \rightarrow \infty$  in equation (7), we obtain equation (8). The unknown coefficients  $C_n^{TM}$  given by equations (4)–(8) are consistent with [26–28]. In the far zone, the z-component of the scattered electric field can be found from equation (2) using the asymptotic

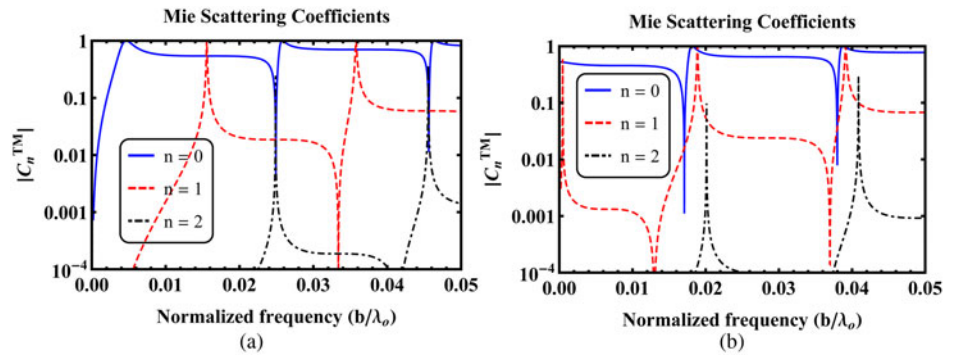


**Fig. 2.** The magnitude of the first three Mie scattering coefficients  $|C_n^{TM}|$  as a function of normalized frequency  $b/\lambda_0$  for (a) BST cylindrical rod and (b) BST coated PEC cylindrical rod for  $n=0, 1$ , and 2. The proposed scattering coefficients for the BST rod are in good agreement with those reported by Vynck et al. [20].

expansion of Hankel function for large argument as given in [27]. Using this far zone scattered electric field in the standard definition of scattering width  $\sigma^{TM}$  [27], one can write the normalized scattering width  $\sigma_N$  as below,

$$\sigma_N = \frac{\sigma^{TM}}{\lambda_1} = \frac{2}{\pi} \left| \sum_{n=-\infty}^{n=+\infty} C_n^{TM} e^{jn(\phi-\phi_0)} \right|^2 \quad (9)$$

where  $\lambda_1$  is the wavelength in the background medium. For sake of convenience, the azimuth angle  $\phi_0$  is assumed to be zero for the current study.

### Effective parameters of a metamaterial composed of dielectric coated conducting rods

In this section, we consider a composite material which consists of an infinite two dimensional periodic arrangements of these dielectric coated PEC cylindrical rods. The background medium is taken to be the free space. All the rods are assumed to be parallel to the  $z$ -axis. The spacings among rods along  $x$  and  $y$ -axes are taken to be  $d$ . Its geometrical configuration has been given in the lower panel of Fig. 1. For the homogenized description of an artificial material containing dielectric coated conducting rods, it is required to satisfy two conditions, i.e.  $k_0 b \ll 1$  and  $k_0 d < 2\pi$ . If these two conditions are satisfied then an artificial material composed of these cylindrical rods can be homogenized. In this way, we can assign the effective permittivity and effective permeability, i.e. effective parameters to such an artificial material. It should be noted that the condition  $k_0 d < 2\pi$  can be used only if the incident wave is normal as the case under study. In the present study, we have taken normal TM incidence. On the other hand, for the oblique angles of incidence, the second necessary condition become  $k_0 d < \pi$  instead of  $k_0 d < 2\pi$ .

It can be seen that if the dielectric coated conducting rod is thin, i.e.  $k_0 b \ll 1$  then the dominant Mie scattering coefficients  $C_n^{TM}$  as given by equations (4)–(8) exists only for  $n=0$  and  $n=1$ . On the other hand, the higher order Mie scattering coefficients for  $n>1$  become negligible for thin rods. Therefore, for the homogenized description of an artificial medium containing dielectric coated conducting rods, it is desired to take only leading Mie scattering coefficients, i.e.  $C_0^{TM}$  and  $C_1^{TM}$ . To justify this statement, it is assumed that the dielectric coating is assumed to be made of a nonmagnetic and ferroelectric ceramic material, i.e.  $\text{Ba}_{0.5}\text{Sr}_{0.5}\text{TiO}_3$  (BST) [19]. It has a relative permittivity of 600 at microwave frequencies and at room temperature. The magnitude of the first three Mie scattering coefficients  $C_n^{TM}$  for the BST cylindrical rod and BST coated conducting cylindrical rod is shown

in Fig. 2. In this case, both types of rods have the same radius of  $b = (0.68/3)(\lambda_0/4)$  at an operating free space wavelength of 25 mm. For the BST coated conducting rod, the inner radius  $a$  of the conducting rod is assumed to be  $b/2$ . It is found from Fig. 2 that for both types of rods, the higher order Mie scattering coefficients which also represent the higher order multipole moments for  $n>1$  induce spectrally narrow features near their resonance frequencies and can be ignored. It is argued that the lowest order Mie scattering coefficient  $C_0^{TM}$  is responsible for an induced electric dipole moment whereas the Mie scattering coefficient  $C_1^{TM}$  is responsible for an induced magnetic dipole moment.

Using the procedure as outlined in [18,20] and taking the incident electric field aligned along the  $z$ -axis and the incident magnetic field along the  $y$ -axis, the electric polarizability per unit length  $Y_e^{zz}$  and the magnetic polarizability per unit length  $Y_m^{yy}$  can be computed using the following relations,

$$Y_e^{zz} = 4j \frac{C_0^{TM}}{k_0^2} \quad Y_m^{yy} = 4j \frac{C_1^{TM}}{k_0^2} \quad (10)$$

Once the electric and magnetic polarizabilities per unit length of an isolated dielectric coated conducting rod are known then the effective parameters, i.e. effective permittivity  $\epsilon_{zz}$  and effective permeability  $\mu_{yy}$  can be found using the non-local homogenization approach given in [12,18]. Thus, the effective permittivity and effective permeability of an artificial material or a metamaterial composed of dielectric coated conducting rods can be written as,

$$\epsilon_{zz} = 1 + \frac{n}{(Y_e^{zz})^{-1} - C_{zz}^{int}} \quad (11)$$

$$\mu_{yy} = 1 + \frac{n}{(Y_m^{yy})^{-1} - C_{yy}^{int}} \quad (12)$$

where  $n = 1/d^2$ . The factors  $C_{zz}^{int}$  and  $C_{yy}^{int}$  represent the  $zz$ - and  $yy$ -components of the dynamic interaction dyadic given by Silverinha [18].

### Numerical results

In the first part of the numerical results, the normalized scattering widths of dielectric coated conducting rods with various realistic dielectric materials have been studied. The scattering widths of these dielectric coated conducting rods have also been compared

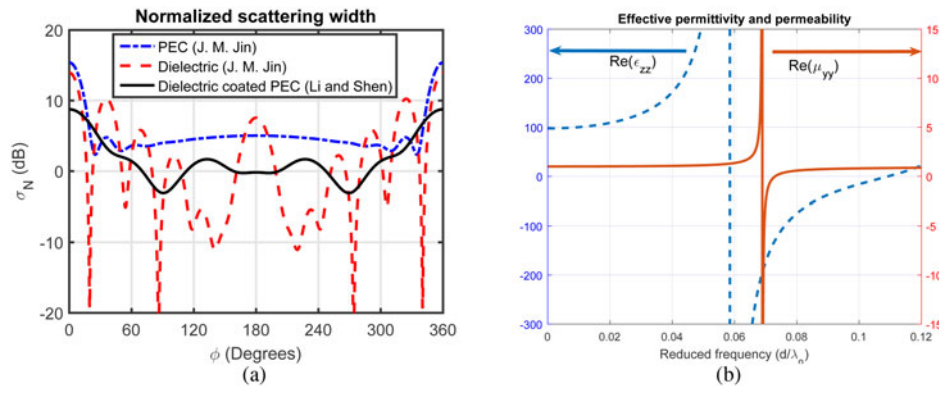


**Fig. 3.** (a) The normalized scattering widths of PEC, dielectric, and dielectric coated PEC cylindrical rods. The electrical and geometrical parameters of PEC and dielectric cylinders or cylindrical rods have been taken from [28] and from [26] in case of the dielectric coated cylindrical rod. These normalized scattering widths are in good agreement with [26,28]. (b) The real parts of the effective permittivity and permeability of a metamaterial composed of BST cylindrical rods based upon the proposed formulation and are found to be in good agreement with those reported by Vynck *et al.* [20]. All these agreements with reported works validate the proposed theory.

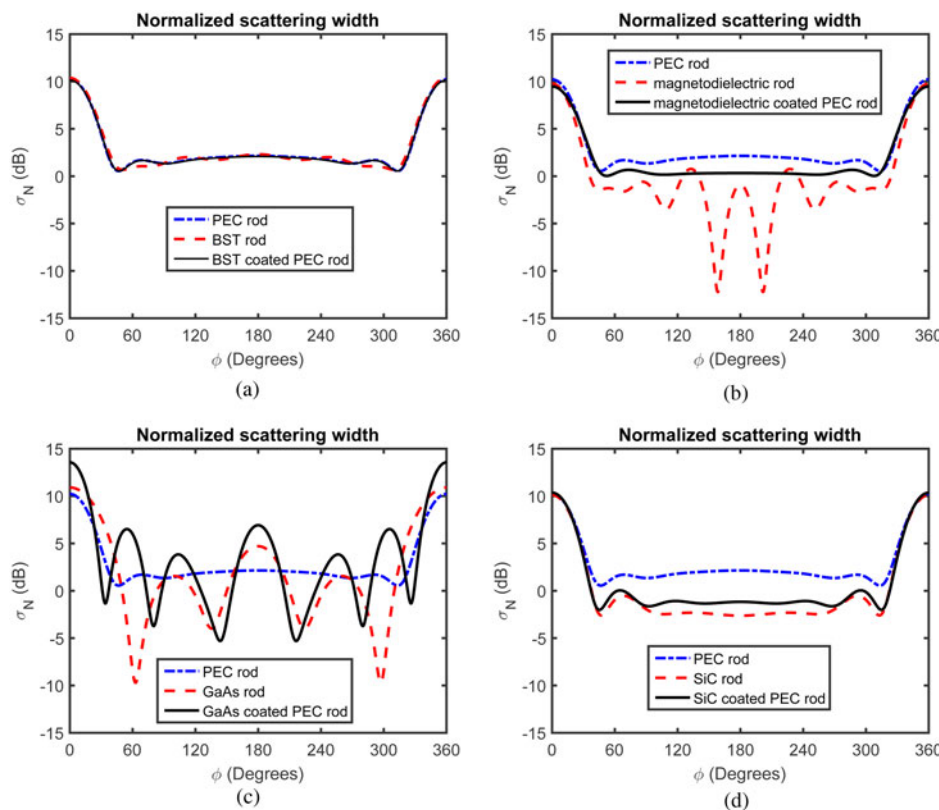


**Fig. 4.** The normalized scattering widths of (a) BST and BST coated PEC cylindrical rods, (b) magnetodielectric and magnetodielectric coated PEC rods, (c) GaAs and GaAs coated PEC rods, and (d) SiC and SiC coated PEC rods and their comparisons with the normalized scattering width of a PEC rod. Here for all the considered cylindrical rods including various material rods, material coated PEC rods and PEC rod, an outer radius of  $b = 50$  mm has been assumed. In case of material coated PEC rods, an inner core radius of the PEC material is taken to be  $a = 0.5b$ .

with the scattering widths of dielectric and PEC rods having the same radii. The types of assumed realistic dielectric materials are  $\text{Ba}_{0.5}\text{Sr}_{0.5}\text{TiO}_3$  (BST) [19], magnetodielectric [29], low loss gallium arsenide (GaAs) [30], and silicon carbide (SiC) [31]. A BST material has a relative permittivity of nearly 600 and is non-magnetic. A magneto-dielectric material has  $\epsilon_{rc} = 13.8 - j0.1$  and  $\mu_{rc} = 11$ . Its relative permittivity is different from unity that is why it is called magnetodielectric. These values are chosen because a low loss garnet material with these parameters can be obtained relatively inexpensively. This material is commercially available in the form of aluminum doped ferrite. The relative permittivity and permeability of a low loss GaAs are taken to be  $\epsilon_{rc} = 12.88 - j0.0004$  and  $\mu_{rc} = 1$  respectively. A SiC is a kind of traditional wave-absorbing materials with high strength and hardness, good corrosion resistance, high thermal stability and

thermal conductivity, and excellent dielectric property. Moreover, the SiC material shows a good absorbing property in the microwave regime. These properties make it a good candidate for the microwave-absorbing materials. For the present analysis, the assumed values of SiC are taken to be  $\epsilon_{rc} \approx 14.2 - j3.8$  and  $\mu_{rc} = 1$ .

In order to validate the proposed formulation presented in Sections “Scattering characteristics of an isolated dielectric coated conducting rod” and “Effective parameters of a metamaterial composed of dielectric coated conducting rods”, the normalized scattering widths of PEC, dielectric, and dielectric coated conducting rods are shown in Fig. 3(a). For PEC and dielectric rods, the radii are taken to be  $\lambda_0$  and the relative permittivity for a non-magnetic dielectric cylinder is taken to be 4. These parameters have been taken from Jin [28]. For a dielectric coated conducting rod, it is assumed that the radius of the inner PEC

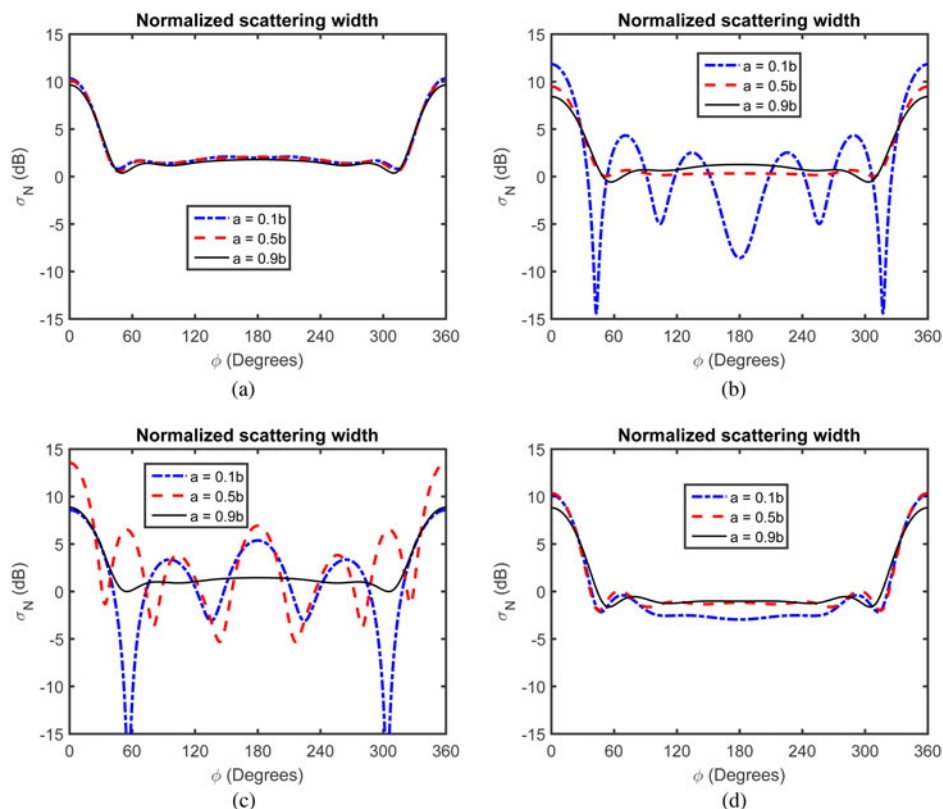


**Fig. 5.** The normalized scattering widths of (a) BST coated PEC rod, (b) magnetodielectric coated PEC rod, (c) GaAs coated PEC rod, and (d) SiC coated PEC rod. For all these cases, the coated rods have an outer radius of  $b = 50$  mm whereas an inner radius  $a$  of a PEC cylindrical rod is variable.

cylinder is 50 mm whereas the radius of outer dielectric cylinder is 100 mm at an operating frequency of 1 GHz. In this case, the relative permittivity of non-magnetic dielectric coating is 9.8 [26]. From Fig. 3(a), it is found that the normalized scattering width (NSW) results are in good agreement with those reported in [26,28]. Likewise, Fig. 3(b) deals with the real parts of the effective permittivity and permeability of a medium composed of BST rods [20]. In this case, the real parts of the effective permittivity and permeability as a function of reduced frequency  $d/\lambda_0$  have been shown and are consistent with those reported by Vynck et al. [20]. It should be noted that the truncation index criteria for summation appearing in equation (9) has been adopted from Li and Shen [26]. For the numerical results of the normalized scattering width shown in Figs 4 and 5, an operating frequency of 3 GHz has been assumed. In these figures, the radii of all types of cylindrical rods are taken to be  $b = 50$  mm. Here NSW for a PEC rod has been used only for comparison. It should be noted that here  $\sigma_N(\phi = 0^\circ)$  corresponds to the normalized forward scattering width (NFSW) whereas  $\sigma_N(\phi = 180^\circ)$  represents the normalized backward scattering width (NBSW). The forward scattering width has applications in point to point communications whereas the backward scattering width is important for radar related communication problems. In case of dielectric coated conducting rods considered in Fig. 4, the inner radius of the PEC core is  $a = 0.5b$ . It is clear from Fig. 4(a) that the normalized scattering patterns for PEC, BST, and BST coated PEC cylindrical rods are nearly the same. This is because the relative permittivity of the BST material is very high and it seems to behave like a PEC material. It is seen that the scattering width pattern of a magnetodielectric material rod is fluctuating having NFSW = 9.78 dB and NBSW = -0.92 dB. It is clear from Fig. 4(b). In this case, the minimum value of NSW is -12.22 dB which

occurs at angles  $\phi = 158.4$  and  $201.6^\circ$ . In case of the magnetodielectric coated conducting rod, the NFSW slightly decreases and becomes 9.47 whereas its NBSW increases to a value of 0.33 dB as compared to their respective values of the magnetodielectric rod. In case of GaAs and GaAs coated conducting rods, it is found that the scattering patterns are fluctuating. In case of the GaAs rod, the NFSW is 10.90 dB and NBSW is 4.70 dB. The minimum value of NSW for a GaAs rod comes out to be -9.70 dB which occurs at  $\phi = 62.8$  and  $297.2^\circ$ . For a GaAs coated conducting rod, the values of NFSW and NBSW increase as compared to a GaAs rod without having an inner PEC core. Thus, it is found from Fig. 4(c) that NFSW = 13.55 dB and NBSW = 6.92 dB for a GaAs coated conducting rod. As we know that the loss tangent of the SiC material is relatively large, therefore, it is seen from Fig. 4 (d) that the scattering patterns of SiC and SiC coated conducting rods are not very much fluctuating. In case of the SiC rod, we found that NFSW is 10.11 dB and NBSW is equal to -2.62 dB. In case of a SiC coated PEC rod, there exists slight enhancements in NFSW and NBSW as compared to a SiC rod which are 10.35 and -1.16 dB respectively. From Table 1, it is concluded that the highest value of NFSW is found for a GaAs coated conducting rod and the lowest value of NFSW is observed in case of magnetodielectric coated conducting rod. Likewise, the highest value of NBSW is observed for a GaAs coated conducting rod and the lowest value of NBSW is found for SiC rod. The influences of inner core radius  $a$  of a PEC rod upon the scattering pattern for various types of dielectric coated conducting rods are shown in Fig. 5. It is found from Fig. 5(a) that for a BST coated conducting rod, the scattering pattern is almost independent of the variation of the inner core radius  $a$ , i.e.  $a = 0.1, 0.5$ , and  $0.9b$ . This is because of the high value of the relative permittivity of the BST material. It is seen from Fig. 5(b) that the scattering pattern for a magnetodielectric coated PEC rod having

**Table 1.** Comparative study of normalized forward and backward scattering widths for various types of cylindrical rods considered in Fig. 4.

Types of rods	NFSW (dB)	NBSW (dB)
PEC rod	10.22	2.15
BST rod	10.37	2.31
BST coated conducting rod	10.14	2.08
Magnetodielectric rod	9.78	-0.92
Magnetodielectric coated conducting rod	9.47	0.33
GaAs rod	10.90	4.70
GaAs coated conducting rod	13.55	6.92
SiC rod	10.11	-2.62
SiC coated conducting rod	10.35	-1.16

$a = 0.1b$  is very much fluctuating. In this case, it is found that the minimum value of the NSW is  $-14.40$  dB for specific angles  $\phi = 42.9$  and  $317.1^\circ$ . It is argued that for these specific angles, the scattered field from the inner PEC rod destructively interferes with the scattered field of magnetodielectric coating. In this case, NFSW is  $11.83$  dB whereas NBSW is  $-8.57$  dB. It is further studied that as the value of  $a$  increases to  $0.5$  and  $0.9b$  then the value of NFSW decreases to  $9.47$  and  $8.41$  dB respectively. Likewise, the values NBSW increases to  $0.32$  and  $1.26$  with the increase of  $a$  from  $0.5b$  to  $0.9b$ . Thus, it is concluded that by expanding the inner core of PEC cylinder inside the magnetodielectric coated conducting rod, the NFSW can be reduced whereas its NBSW can be enhanced. It is also observed that for  $a = 0.5$  and  $0.9b$ , the overall scattering pattern is not very much fluctuating in contrast to the scattering

pattern for  $a = 0.1b$ . In Fig. 5(c), the influences of inner core radius  $a$  upon the scattering width of a GaAs coated conducting rod have been shown. It is studied that for  $a = 0.1b$ , the overall scattering pattern is fluctuating with the NFSW =  $8.57$  dB and NBSW =  $5.37$  dB. The minimum value of the scattering width is found to be  $-20$  dB which occurs at angles  $\phi = 56.25$  and  $303.75^\circ$ . Therefore, it is concluded that the GaAs coating can be used to significantly reduce the scattering width of a small radius PEC cylindrical rod at specific scattering or observation angles. As the value of the inner core radius increases to  $a = 0.5b$ , it enhances the NFSW as well as the NBSW as compared to the respective NSW values in the case of  $a = 0.1b$ . In this case, we have NFSW =  $13.56$  dB and NBSW =  $6.92$  dB. For  $a = 0.9b$ , i.e. the GaAs coating layer is very thin then the values of NFSW and NBSW become closer to the corresponding values of the PEC cylindrical rod having radius  $b$ , i.e. NFSW =  $8.90$  dB and NBSW =  $1.44$  dB. In case of the SiC coated conducting rod, it is observed that the maximum value of NFSW is  $10.35$  dB which exists for  $a = 0.5b$  whereas the minimum value of NFSW which is equal to  $-2.95$  dB occurs for  $a = 0.1b$ . This is clear from Fig. 5(d).

In the second part of numerical results, we investigate the effective parameters of a metamaterial composed of dielectric coated conducting rods and their comparisons with the respective effective parameters of metamaterials composed of dielectric and PEC rods. These effective parameters are shown in Figs 5-9. The types of considered dielectric coatings are BST, magnetodielectric, GaAs, and SiC. For all these Figs 7-9, it is assumed that  $b = (0.68d)/3$  for lattice spacing of  $d = 25$  mm. This value of  $b$  has been adopted from [20] with  $a = 0.01b$ . The significance of the chosen value of  $a = 0.01b$  has been discussed in the last paragraph of this section. In case of a metamaterial composed of PEC rods, the low frequency plasmonic epsilon negative BW which

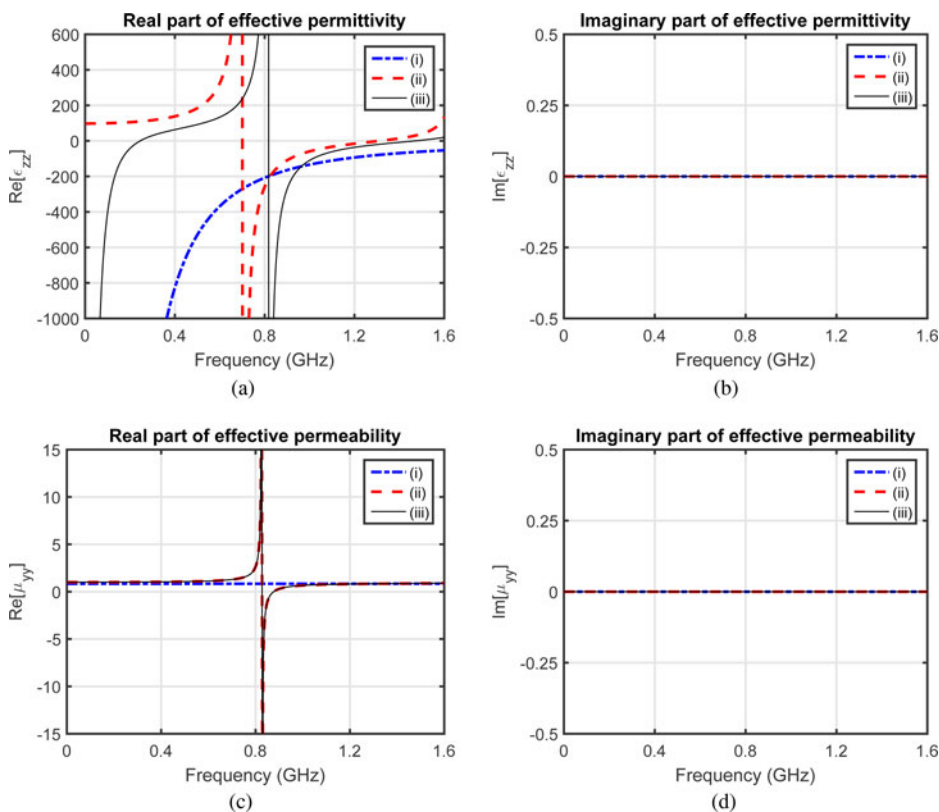


**Fig. 6.** The (a) real and (b) imaginary parts of the effective permittivity  $\epsilon_{zz}$  and (c) real and (d) imaginary parts of the effective permeability  $\mu_{yy}$  of artificial materials or metamaterials composed of (i) PEC rods (ii) BST rods and (iii) BST coated PEC rods.

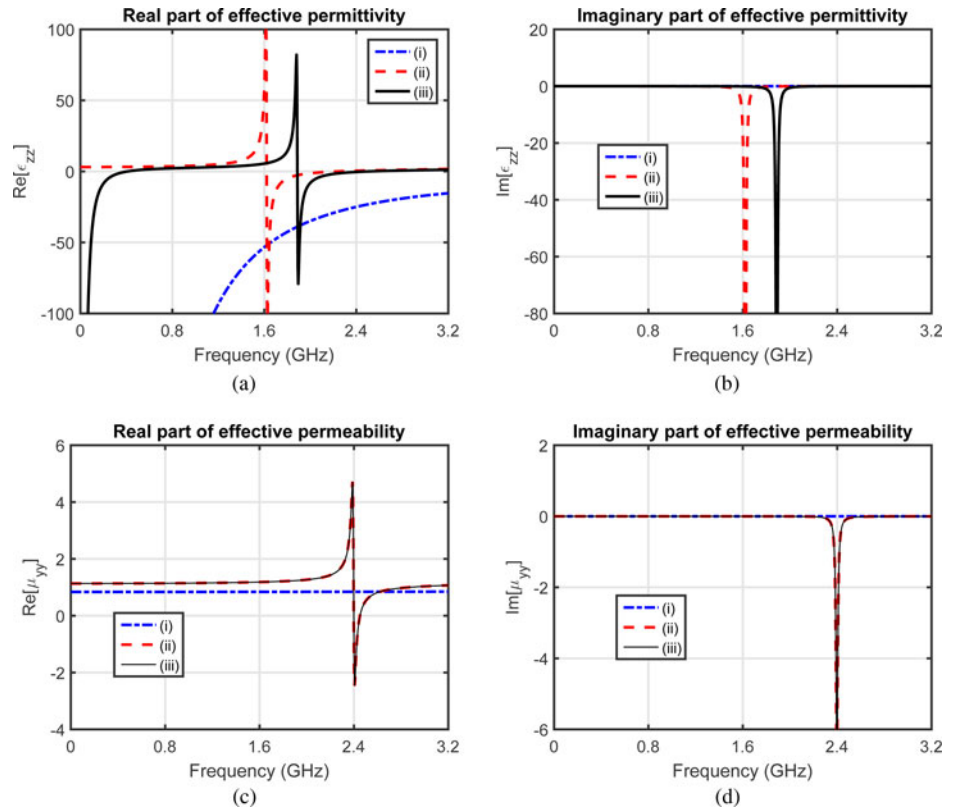


**Fig. 7.** The (a) real and (b) imaginary parts of the effective permittivity and (c) real and (d) imaginary parts of the effective permeability of metamaterials composed of (i) PEC rods, (ii) magnetodielectric rods, and (iii) magnetodielectric coated PEC rods.

extends from zero frequency to plasma frequency  $f_p$  comes out to be 6.665 GHz. In this case, we have the plasma frequency of 6.665 GHz. Thus such type of a metamaterial composed of PEC

rods can only be used for an ENG metamaterial and is very well known in the literature. Thus, the effective parameters of a metamaterial composed of PEC rods have been shown in the

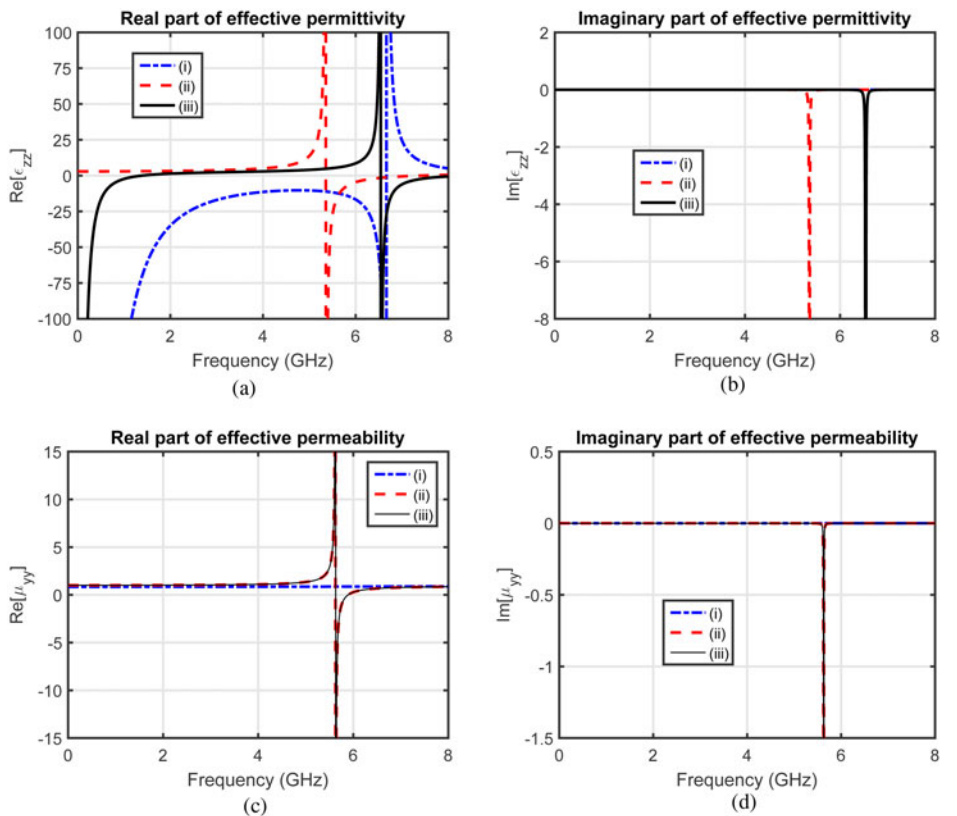


**Fig. 8.** The (a) real and (b) imaginary parts of the effective permittivity and (c) real and (d) imaginary parts of the effective permeability of metamaterials composed of (i) PEC rods, (ii) GaAs rods, and (iii) GaAs coated PEC rods.



next coming figures only for comparison purposes. The effective parameters of metamaterials composed of BST rods and BST coated conducting rods are shown in Fig. 6. In case of a BST rod medium, it is studied that resonance frequency  $f_r^\epsilon = 0.701$  GHz whereas its plasma frequency  $f_p^\epsilon = 1.3122$  GHz. In this case, the resonant ENG BW can be found from  $f_p^\epsilon - f_r^\epsilon$  which is equal to 0.6112 GHz. For a BST coated conducting rod medium, we have  $f_r^\epsilon = 0.8178$  GHz and  $f_p^\epsilon = 1.4689$  GHz. Based upon these frequencies, an ENG bandwidth of 0.6511 GHz has been found. This shows an enhancement of 0.0399 GHz in an ENG bandwidth as compared to an ENG bandwidth of a metamaterial composed of BST rods. This is clear from Fig. 6(a). Also an additional plasmonic ENG bandwidth of 0.2453 GHz has been found in case of a metamaterial composed of BST coated conducting rods. On the other hand, for the real part of the effective permeability of a metamaterial composed of BST rods, it is analyzed that resonance frequency  $f_r^\mu = 0.8278$  GHz and plasma frequency  $f_p^\mu = 0.8767$  GHz. Therefore, an MNG bandwidth of 0.0489 GHz is observed. For a metamaterial composed of BST coated conducting rods, a blueshift in resonance and plasma frequencies has been observed in contrast to a metamaterial composed of BST rods, i.e.  $f_r^\mu = 0.8277$  GHz and  $f_p^\mu = 0.8769$  GHz. Thus, a % increase in the MNG bandwidth of 0.6135% in case of a metamaterial composed of BST coated conducting rods is observed as compared to a metamaterial composed of BST rods. From the above analysis, it is concluded that a metamaterial composed of BST rods has a DNG bandwidth of 0.0489 GHz whereas a metamaterial comprised BST coated conducting rods has a DNG bandwidth of 0.0492 GHz. This shows that a % increase of 0.6135% in a DNG bandwidth for a metamaterial composed of BST coated conducting rods has been observed as compared to a metamaterial composed of only BST rods as given by Vynck and co-workers [20]. From

Figs 6(b) and 6(d), it is seen that the imaginary parts of effective permittivity and effective permeability are zeros as expected because of lossless and non-magnetic natures of the BST and PEC materials.

In Fig. 7, the effective parameters of metamaterials composed of magnetodielectric and magnetodielectric coated conducting rods have been shown. It is studied that for a metamaterial composed of magnetodielectric rods, we have resonance frequency  $f_r^\epsilon = 1.6206$  GHz and plasma frequency  $f_p^\epsilon = 2.2443$  GHz. Therefore, an ENG bandwidth of 0.6237 GHz has been found for a metamaterial composed of magnetodielectric rods. In case of a metamaterial composed of magnetodielectric coated conducting rods, a blueshift in resonance and plasma frequencies has been observed as compared to a metamaterial composed of magnetodielectric rods, i.e.  $f_r^\epsilon = 1.8874$  GHz and  $f_p^\epsilon = 2.5052$  GHz. In this case, we have an ENG bandwidth of 0.6178 GHz. Thus, by an insertion of a very thin PEC rod inside a magnetodielectric rod causes a reduction in an ENG bandwidth. In addition to this, there also exists a plasmonic ENG bandwidth of 0.4096 GHz for a metamaterial composed of magnetodielectric coated conducting rods. The absorption peaks associated with the imaginary parts of the effective permittivity which occur at resonance frequencies of these metamaterials are apparent from Fig. 7(b). It is studied from Figs 7(c)–7(d) that the effective permeability characteristics of metamaterials composed of magnetodielectric and magnetodielectric coated conducting rods are almost identical. In both cases, we have  $f_r^\mu \approx 2.3984$  GHz and  $f_p^\mu \approx 2.4512$  GHz with an MNG bandwidth of 0.0528 GHz. As there exists no overlap among the ENG and MNG bandwidths for a magnetodielectric rodged metamaterial, therefore, no DNG bandwidth exists for a metamaterial composed of magnetodielectric rods. On the other hand, there exists an overlap among the ENG and MNG

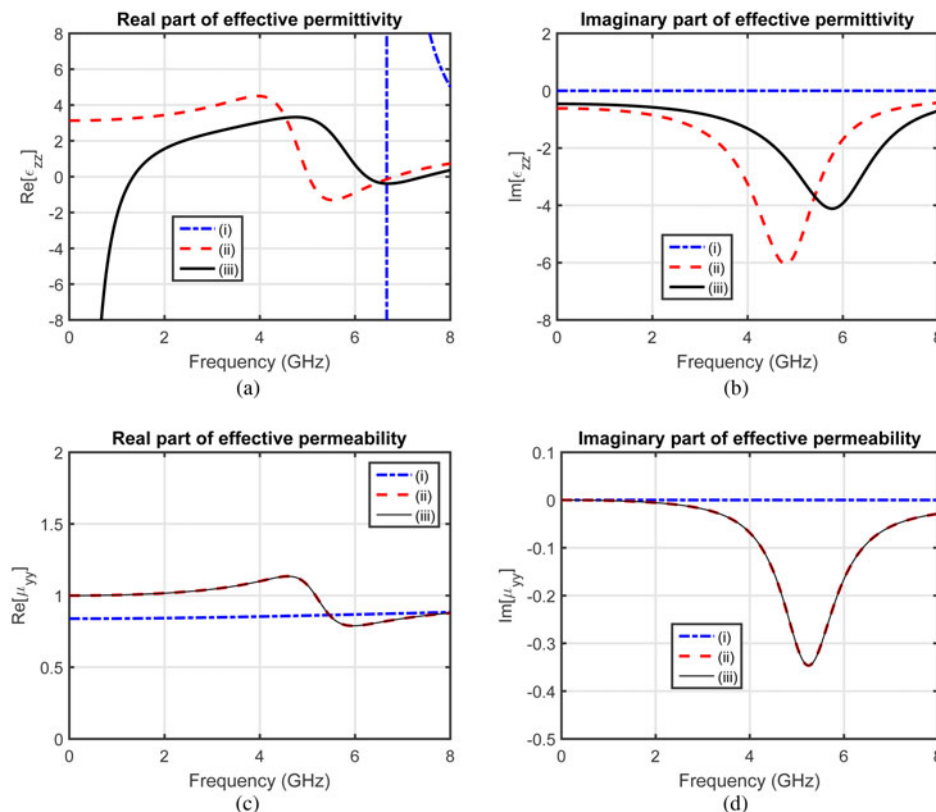


Fig. 9. The (a) real and (b) imaginary parts of the effective permittivity and (c) real and (d) imaginary parts of the effective permeability of metamaterials composed of (i) PEC rods, (ii) SiC rods, and (iii) SiC coated PEC rods.

**Table 2.** Comparative study of plasmonic ENG, resonant ENG, MNG, and DNG bandwidths (BWs) for metamaterials composed of various types of rods considered in Figs 6–9. All the table entries represent the bandwidths in GHz. Here MD is used for magnetodielectric.

Types of rods	Plasmonic ENG	Resonant ENG	MNG	DNG
PEC	6.6650	–	–	–
BST	–	0.6112	0.0489	0.0489
BST coated PEC	0.2453	0.6511	0.0492	0.0492
MD	–	0.6237	0.0528	–
MD coated PEC	0.4096	0.6178	0.0528	0.0528
GaAs	–	2.0690	0.2664	0.2664
GaAs coated PEC	1.3844	1.8781	0.2614	–
SiC	–	1.7932	–	–
SiC coated PEC	1.3414	1.1947	–	–

bandwidths for a metamaterial composed of magnetodielectric coated conducting rods and we have a DNG bandwidth of 0.0528 GHz.

The effective parameters of metamaterials composed of GaAs and GaAs coated conducting rods are shown in Fig. 8. For a metamaterial composed of GaAs rods, we have  $f_r^\epsilon = 5.356$  GHz,  $f_p^\epsilon = 7.425$  GHz,  $f_r^\mu = 5.6249$  GHz, and  $f_p^\mu = 5.8913$  GHz. Using these information, it is argued that the ENG bandwidth is 2.069 GHz and the MNG bandwidth is 0.2664 GHz. In case of a metamaterial composed of GaAs coated conducting rods, a blueshift in resonance as well as plasma frequencies associated with the effective permittivity and effective permeability is observed in contrast to the respective frequencies for a metamaterial composed of GaAs rods. These frequencies become  $f_r^\epsilon = 6.5416$  GHz,  $f_p^\epsilon = 8.4197$  GHz,  $f_r^\mu = 5.631$  GHz, and  $f_p^\mu = 5.8924$  GHz. Thus, we have ENG bandwidth of 1.8781 GHz and MNG bandwidth of 0.2614 GHz. In this case, an additional plasmonic ENG bandwidth of 1.3844 GHz has also been observed. From the above analysis, it is concluded that there exists a DNG bandwidth of 0.2664 GHz for a metamaterial composed of GaAs rods. It is observed that a metamaterial composed of GaAs rods has wider ENG, MNG, and DNG bandwidths. This is because of the relatively large value of the real part of the relative permittivity and very small value of the

loss tangent of the GaAs material. There is no DNG bandwidth for a metamaterial composed of GaAs coated conducting rods. In Fig. 9, the effective parameters of metamaterials composed of SiC rods and SiC coated conducting rods have been shown. A metamaterial composed of SiC rods has  $f_r^\epsilon = 5.0272$  GHz and  $f_p^\epsilon = 6.8204$  GHz which represents an ENG bandwidth of 1.7932 GHz. By inserting a very thin PEC rod having  $a = 0.01b$  as the case under consideration inside this SiC rod at its center, a blueshift in resonance and plasma frequencies has been seen from Fig. 9 (a). Thus, for a metamaterial composed of SiC coated conducting rods, we have  $f_r^\epsilon = 6.2472$  GHz and  $f_p^\epsilon = 7.4419$  GHz which shows an ENG bandwidth of 1.1947 GHz. It is further investigated that for metamaterials composed of SiC and SiC coated conducting rods, no MNG bandwidths exist because of the very large value of the loss tangent associated with the dielectric constant of the SiC material. This is obvious from Fig. 9(c). From Figs 9(b) and 9(d), it is studied that there exists absorption peaks of wider bandwidths associated with the imaginary parts of the effective permittivity and effective permeability. This is because of the inherently increased lossy nature of the SiC material which in turn broadens the absorption peaks. In order to highlight the important findings given in Figs 6–9, a Table 2 is constructed which gives the comparative analysis of plasmonic ENG, resonant ENG, MNG, and DNG bandwidths associated with the considered rodDED metamaterials. From Table 2, some of the important conclusions about optimal designs of metamaterials can be drawn. The widest plasmonic ENG bandwidth is observed in case of a metamaterial composed of PEC rods which is expected whereas the narrowest plasmonic ENG bandwidth is found for a metamaterial composed of BST coated conducting rods. It is further investigated that a wider DNG bandwidth has been observed for a metamaterial composed of BST coated conducting rods in contrast to the corresponding DNG bandwidth of a metamaterial composed of BST rods. A metamaterial composed of magnetodielectric coated conducting rods has overlapping ENG and MNG bandwidths which gives rise to a wider DNG bandwidth as compared to the DNG bandwidth of a metamaterial composed of BST coated PEC rods. Among all the considered metamaterials, the widest ENG, MNG, and DNG bandwidths have been observed in case of a metamaterial composed of GaAs rods. In case of a metamaterial composed of SiC rods, we have only resonant ENG bandwidth whereas for a metamaterial composed of SiC coated conducting rods, we have resonant as well as plasmonic ENG bandwidths. The widest DNG bandwidth in case of a metamaterial composed of coated conducting rods has been observed for a metamaterial composed of magnetodielectric coated conducting rods.

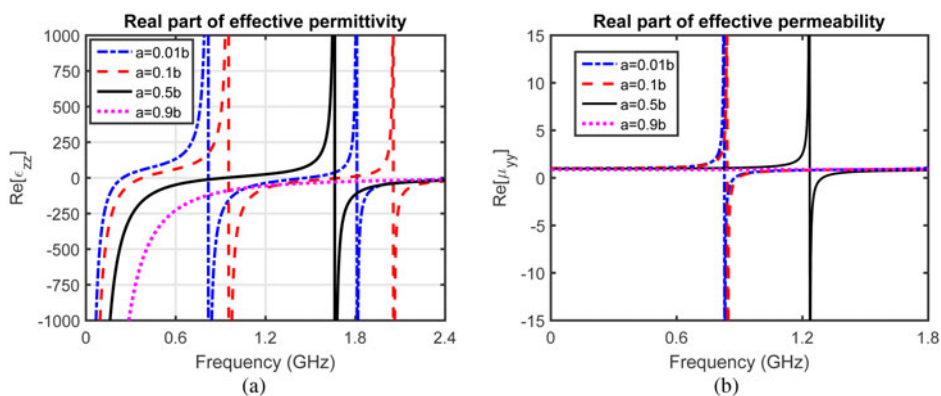


**Fig. 10.** The influences of inner core radius  $a$  of PEC cylinder upon the (a) real part of the effective permittivity  $\epsilon_{zz}$  and (b) real part of the effective permeability  $\mu_{yy}$  of a metamaterial composed of BST coated perfectly conducting rods.

For the present study, one of the crucial parameters is the radius  $a$  of an inner PEC core which significantly modify the effective parameters of a metamaterial composed of dielectric coated conducting rods. The influences of the inner core radius upon the real parts of the effective permittivity and effective permeability of a metamaterial composed of only BST coated conducting rods are shown in Fig. 10. It is already mentioned in Fig. 6 that if  $a = 0.01b$  then there exists a DNG bandwidth for a metamaterial composed of BST coated rods. In this case, the coating layer is relatively thicker whereas the inner core is very thin. As the value of  $a$  increases to  $0.1$ ,  $0.5$ , and  $0.9b$  then there exists no DNG bandwidth for a metamaterial composed of BST coated conducting rods. That is why, we have used  $a = 0.01b$  for all Figs 6–9. This is discussed in detail as below. It is seen that as the value of  $a$  becomes  $0.1$ ,  $0.5$ , and  $0.9b$  then the corresponding plasmonic ENG bandwidth increases to  $0.3772$ ,  $0.9272$  and  $4.9894$  GHz respectively. Likewise, for  $a = 0.1b$ , we have  $f_r^\epsilon = 0.95376$  GHz,  $f_p^\epsilon = 1.7038$  GHz,  $f_r^\mu = 0.8418$  GHz, and  $f_p^\mu = 0.8925$  GHz. Thus, there exists no DNG bandwidth because we have non-overlapping ENG and MNG bandwidths. In this case, we have a ENG bandwidth of  $0.7501$  GHz and a MNG bandwidth of  $0.0507$  GHz. By increasing the inner core radius  $a$  to  $0.5b$ , blue-shift in resonance as well as plasma frequencies has been observed as compared to the respective frequencies for  $a = 0.1b$  case. They become  $f_r^\epsilon = 1.6626$  GHz,  $f_p^\epsilon = 3.164$  GHz,  $f_r^\mu = 1.2348$  GHz, and  $f_p^\mu = 1.2957$  GHz. Thus, we have non-overlapping ENG and MNG bandwidths of  $1.5014$  and  $0.0609$  GHz respectively which signifies that there exists no DNG bandwidth. In the last case of  $a = 0.9b$  there exists no resonant ENG bandwidth and hence no DNG bandwidth. But we have  $f_r^\mu = 5.5142$  GHz and  $f_p^\mu = 5.5758$  GHz which represents an MNG bandwidth of  $0.0616$  GHz.

### Concluding remarks

An analysis about the scattering characteristics of an isolated dielectric coated PEC rods have been given by assuming realistic material coatings. These realistic materials are BST, GaAs, magnetodielectric, and SiC. It is found that the GaAs coating can be used to significantly reduce the scattering width of a thin PEC cylindrical rod at specific observation angles. It is also observed that by increasing the inner core radius of the PEC rod inside the magnetodielectric coated conducting rod, the NFSW can be diminished whereas its NBSW can be enhanced. Based upon the scattering characteristics of an individual coated conducting rod, the problem is further extended to calculate the effective parameters of a metamaterial composed of coated conducting rods using nonlocal homogenization theory. During the study, it is found that the widest plasmonic ENG bandwidth is observed in case of a metamaterial composed of PEC rods whereas the narrowest plasmonic ENG bandwidth is found for a metamaterial composed of magnetodielectric coated conducting rods. A % increase of  $0.6135\%$  in a DNG bandwidth for a metamaterial composed of BST coated conducting rods has been observed as compared to a metamaterial composed of only BST rods which were reported previously by Vynck and co-workers. Also an additional plasmonic ENG bandwidth has been found in case of a metamaterial composed of BST coated conducting rods. It is shown that a metamaterial composed of MD coated conducting rods has the wider DNG bandwidth as compared to metamaterials composed of BST rods and BST coated conducting rods. It is further studied that the widest ENG, MNG, and DNG bandwidths have been observed in case of a metamaterial

composed of GaAs rods. The narrowest ENG, MNG, and DNG bandwidths have been observed for metamaterials composed of BST rods as reported by Vynck and co-workers. It is further observed that by increasing the inner core radius of BST coated conducting rods we can increase the plasmonic ENG bandwidth. The presented parametric analysis is helpful in designing of ENG, MNG, and DNG metamaterials composed of coated conducting cylindrical rods.

### References

1. Veselago VG (1968) The electrodynamics of substances with simultaneously negative values of  $\epsilon$  and  $\mu$ . *Soviet Physics Uspekhi*, **10**, 509–514.
2. Pendry JP, Holden AJ, Stewart WJ and Youngs I (1996) Extremely low frequency plasmons in metallic mesostructures. *Physical Review Letters*, **76**, 4773–4776.
3. Pendry JP, Holden AJ, Robbins DJ and Stewart WJ (1999) Magnetism from conductors and enhanced nonlinear phenomena. *IEEE Transactions on Microwave Theory and Techniques*, **47**, 2075–2084.
4. Smith DR, Padilla WJ, Vier DC, Nemat-Nasser SC and Schultz S (2000) Composite medium with simultaneously negative permeability and permittivity. *Physical Review Letters*, **84**, 4184–4187.
5. Shelby RA, Smith DR and Schultz S (2001) Experimental verification of a negative index of refraction. *Science*, **292**, 77–79.
6. Alu A and Engheta N (2004) Guided modes in a waveguide filled with a pair of single-negative (SNG), double-negative (DNG), and/or double-positive (DPS) layers. *IEEE Transactions on Microwave Theory and Techniques*, **52**, 199–210.
7. Alu A and Engheta N (2003) Pairing an epsilon-negative slab with a mu-negative slab: resonance, tunneling and transparency. *IEEE Transactions on Antennas and Propagation*, **51**, 2558–2571.
8. Alu A and Engheta N (2005) Polarizabilities and effective parameters of collections of spherical nanoparticles formed by pairs of concentric double-negative (DNG), single-negative (SNG) shells, and/or double-positive (DPS) metamaterial layers. *Journal of Applied Physics*, **97**, 094310-1–12.
9. Engheta N, Alu A, Silveirinha MG, Salandrino A and Li J (2006) DNG, SNG, ENZ and MNZ metamaterials and their potential applications. *IEEE MELECON*, Benalmadena, Spain, May 16–19.
10. Kshetrimayum RS (2004) A brief intro to metamaterials. *IEEE Potentials*, **23**, 44–46.
11. Awan ZA (2014) Reflection and transmission properties of a wire grid embedded in a SNG or SZ medium. *Journal of Modern Optics*, **61**, 1147–1151.
12. Awan ZA (2015) Nonlocal effective parameters of a coated sphere medium. *Journal of Modern Optics*, **62**, 528–535.
13. Belov PA, Tretyakov SA and Viitanen AJ (2002) Dispersion and reflection properties of artificial media formed by regular lattices of ideally conducting wires. *Journal of Electromagnetic Waves and Applications*, **16**, 1153–1170.
14. Awan ZA (2014) Imperfections for an equivalent surface impedance of a uniaxial wire medium. *Journal of Electromagnetic Waves and Applications*, **28**, 1834–1855.
15. Machac J, Protiva P and Zehentner J (2007) Isotropic epsilon-negative. *IEEE/MTT-S International Microwave Symposium*, Honolulu, HI, USA, June 3–8, pp. 1–4.
16. Awan ZA and Rizvi AA (2013) Random errors for a nonlocal epsilon negative medium. *Optics Communications*, **295**, 239–248.
17. Awan ZA and Rizvi AA (2013) Positional disorder for a medium composed of loaded wire dipoles. *Optics Communications*, **309**, 338–343.
18. Silveirinha MG (2006) Nonlocal homogenization model for a periodic array of  $\epsilon$  negative rods. *Physical Review E*, **73**, 046612-1–10.
19. Peng L, Ran L, Chen H, Zhang H, Kong JA and Grzegorzczak TM (2007) Experimental observation of left-handed behavior in an array of standard dielectric resonators. *Physical Review Letters*, **98**, 157043-1–4.
20. Vynck K, Felbacq D, Centeno E, Căbuz AI, Cassagne D and Guizal B (2009) All-dielectric rod-type metamaterials at optical frequencies. *Physical Review Letters*, **102**, 133901-1–4.

21. **Peng L, Ran L and Mortensen NA** (2010) Achieving anisotropy in metamaterials made of dielectric cylindrical rods. *Applied Physics Letters*, **96**, 241108-1-3.
22. **Li Y and Ling H** (2010) Investigation of wave propagation in a dielectric rod array: toward the understanding of HF/VHF propagation in a forest. *IEEE Transactions on Antennas and Propagation*, **58**, 4025-4032.
23. **Valero FJV and Vesperinas MN** (2012) Composite of resonant dielectric rods: a test of their behavior as metamaterial refractive elements. *Photonics and Nanostructures: Fundamentals and Applications*, **10**, 423-434.
24. **Valagiannopoulos CA and Tretyakov SA** (2014) Symmetric absorbers realized as gratings of PEC cylinders covered by ordinary dielectrics. *IEEE Transactions on Antennas and Propagation*, **62**, 5089-5098.
25. **Giovampaola CD and Engheta N** (2014) Digital metamaterials. *Nature Materials*, **13**, 1115-1121.
26. **Li C and Shen Z** (2003) Electromagnetic scattering by a conducting cylinder coated with metamaterials. *Progress in Electromagnetics Research*, **42**, 91-105.
27. **Balanis CA** (1989) *Advanced Engineering Electromagnetics*. New York: Wiley.
28. **Jin JM** (2015) *Theory and Computation of Electromagnetic Fields*. New Jersey: Wiley.
29. **Shore RA and Yaghjian AD** (2006) *Traveling Waves on Two and Three-Dimensional Periodic Arrays of Lossless Acoustic Monopoles, Electric Dipoles, and Magnetodielectric Spheres* (Rep. AFRL-SN-HS-TR-2006-0039). Air Force Res. Lab: Hanscom Air Force Base, MA, pp. 1-203.
30. **Seeger K** (1988) Microwave dielectric constants of silicon, gallium arsenide, and quartz. *Journal of Applied Physics*, **63**, 5439-5443.
31. **Kuang J and Cao W** (2013) Silicon carbide whiskers: preparation and high dielectric permittivity. *Journal of American Ceramic Society*, **96**, 2877-2880.



**Zeshan Akbar Awan** received a Ph.D. degree in Electronics from the Quaidi-Azam University, Islamabad, Pakistan in 2013. He is presently an assistant professor at the same university. He has worked as a Post-Doctoral candidate within LEOST Laboratory of the COSYS department in IFSTTAR, Lille, France from January to July 2018. He has authored or co-authored many research articles. His research interests include metamaterials, metasurfaces, and antenna theory.



**Hassn Ullah** received his Master of philosophy degree in Electronics from Quaid-i- Azam University, Islamabad, Pakistan. He is currently pursuing his Ph.D. degree in Electronics from the same university. His main research interest includes electromagnetic meta-materials, electromagnetic scattering from dielectric objects with applications in remote sensing.



**Ahsan Ullah** received his Masters degree in Electronics from Quaid-i-Azam University Islamabad, Pakistan in 2016. He has also received his MPhil degree in Electronics from the same university in 2018. His main areas of research include electromagnetic scattering and metamaterials.



**Afshan Ashraf** received his Masters degree in Electronics from Quaid-i-Azam University Islamabad, Pakistan in 2016. He has also received his MPhil degree in Electronics from the same university in 2018. His main areas of research include chiral and bi-isotropic media and electromagnetic scattering.